Supplementary Information

Electrosynthesis of Ruthenium Nanocluster Incorporated Nickel Diselenide for Efficient Overall Water Splitting

Vipin Yadav[a], Megha[b], Prasenjit Sen[*b] and M. M. Shaijumon[*a]

[a] *School of Physics, Indian Institute of Science Education and Research Thiruvananthapuram, Maruthamala PO, Thiruvananthapuram, Kerala 695551, India.*

Email: shaiju@iisertvm.ac.in

[b] *Harish-Chandra Research Institute, HBNI, Chhatnag Road, Jhunsi, Allahabad, 211019, India.*

Email: prasen@hri.res.in

Contents:

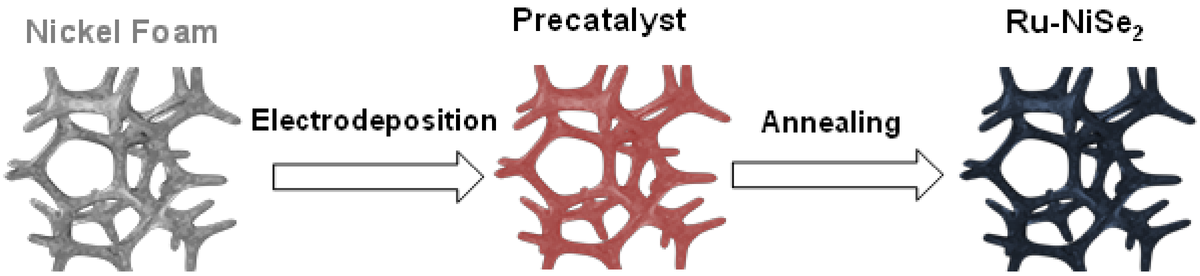

Fig. S1. Schematic illustration of the electrosynthesis of ruthenium cluster decorated nickel diselenide supported on nickel foam (Ru-$NiSe_2$).

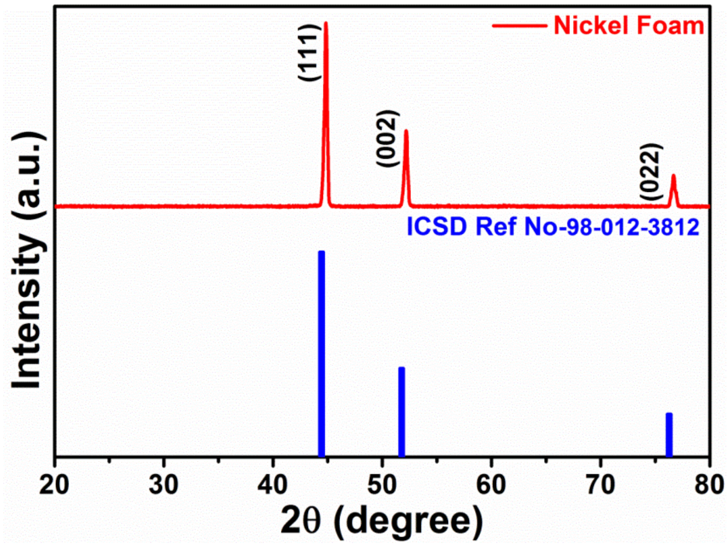

Fig. S2. XRD pattern of bare nickel foam with corresponding plans of (111), (002), and (022) at respective 2 theta angles.

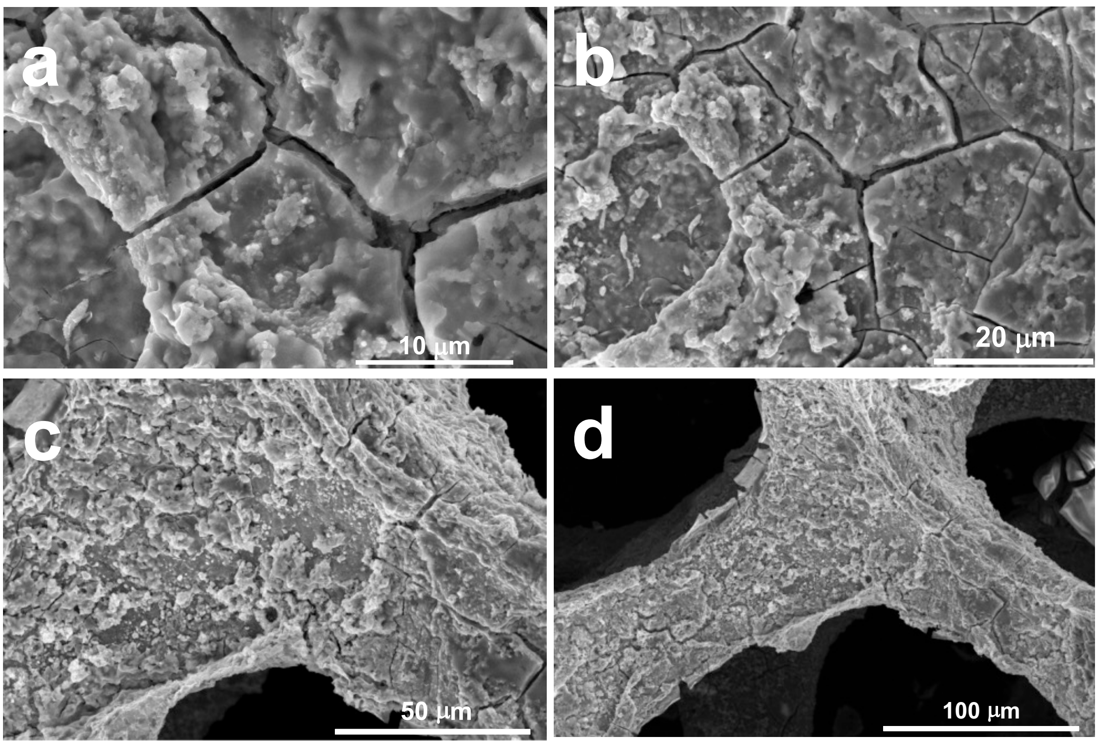

Fig. S3. SEM image of electrodeposited $NiSe_2$ sample over NF at different magnifications.

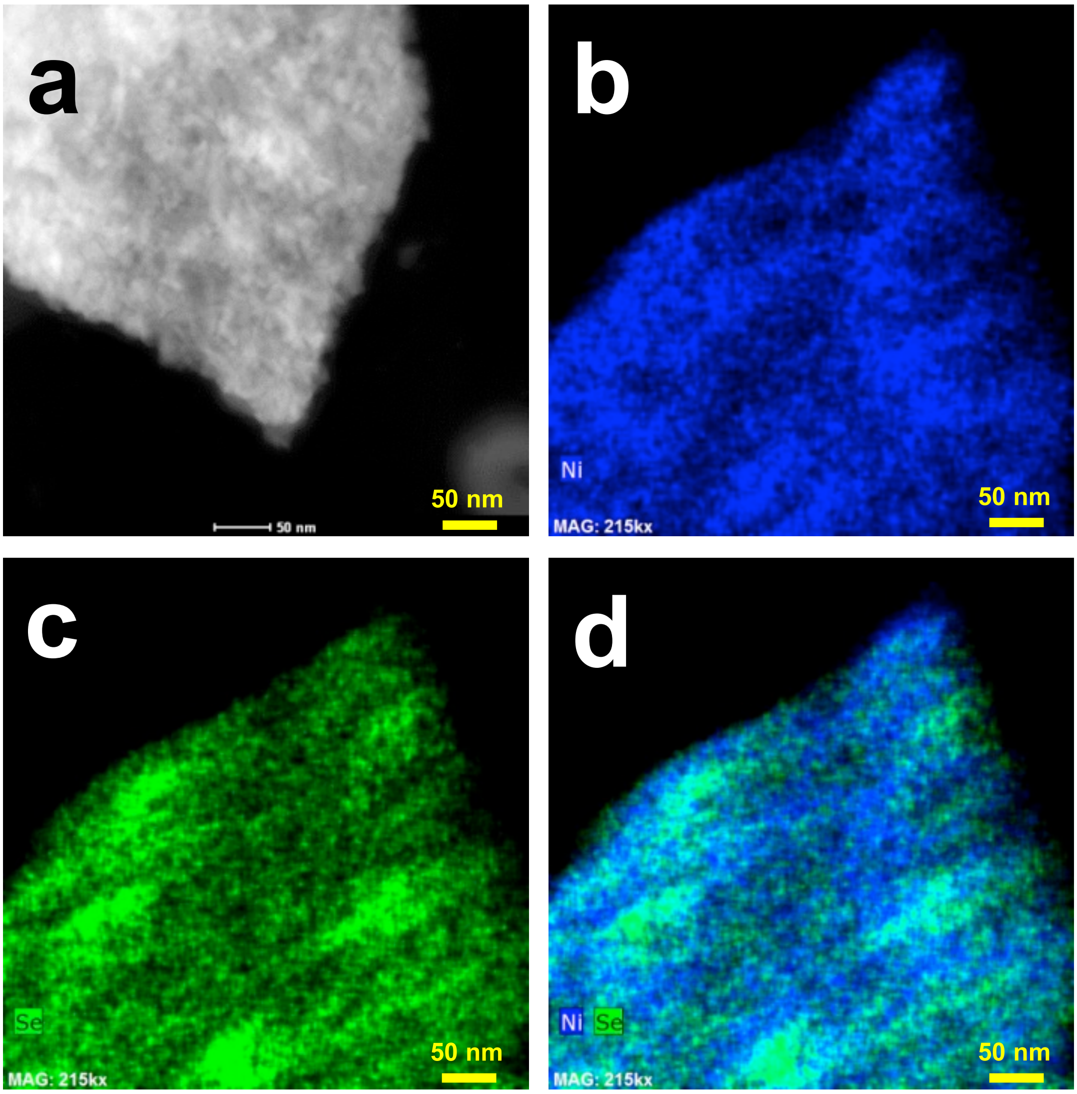

Fig. S4. EDAX mapping. (a) Field Image of $NiSe_2$, (b) elemental mapping of nickel, (c) elemental mapping of selenium, (d) merge of both images (b) and (c).

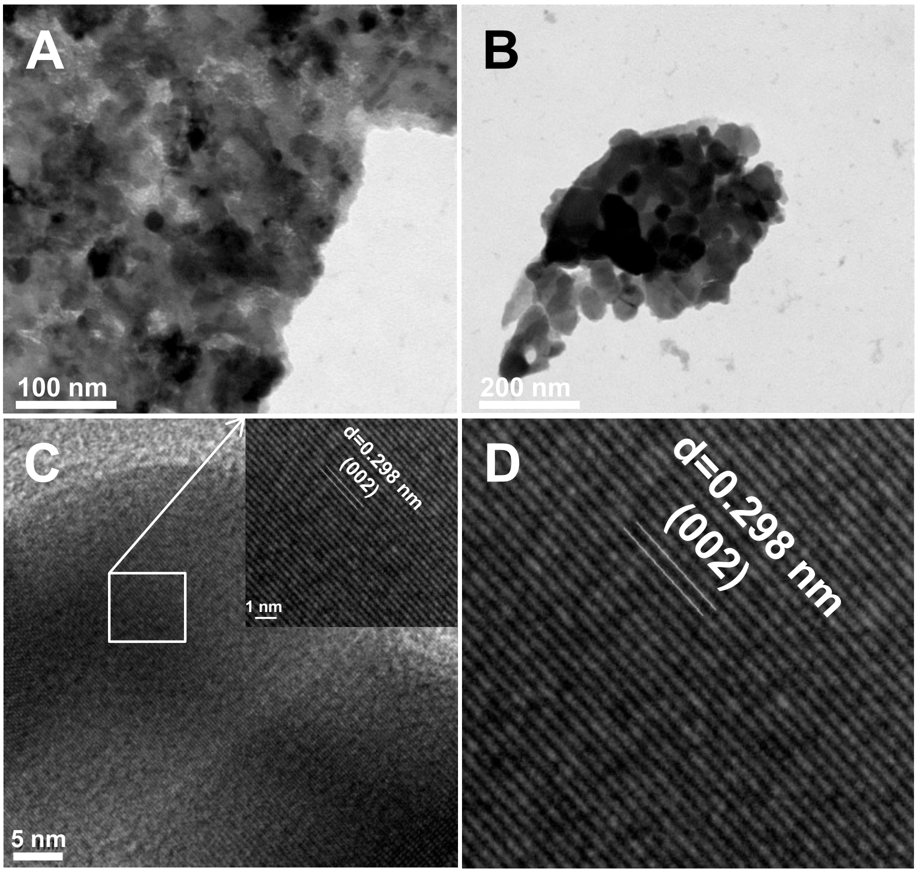

Fig. S5. TEM images (a-b) low magnification, and (c-d) high magnification TEM images of $NiSe_2$.

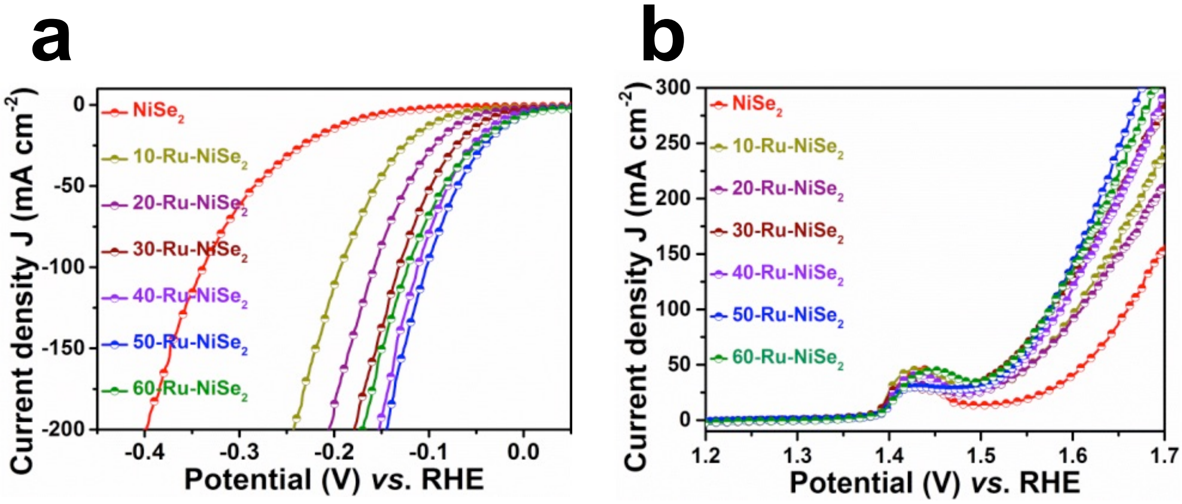

Fig. S6. HER and OER LSV. (a) HER LSV plots, and (b) OER LSV plots of prepared electrodes measured at a scan rate of 2 mV sec^{-1} in 1.0 M KOH.

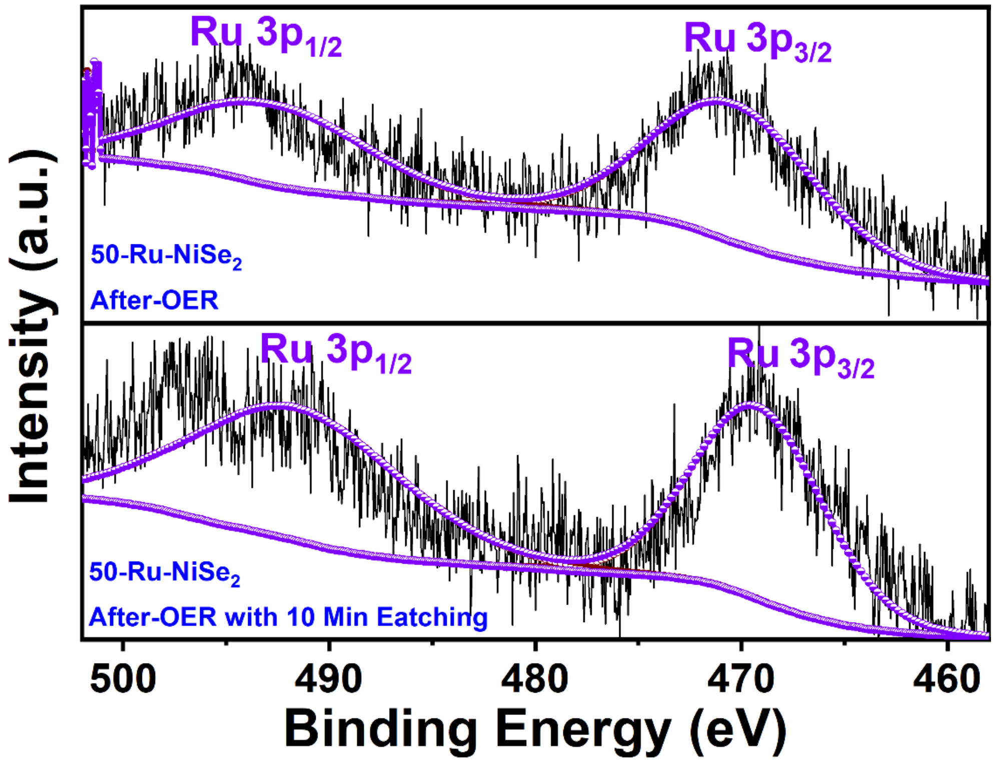

Fig. S7. Post XPS Analysis of ruthenium 3p after OER stability test.

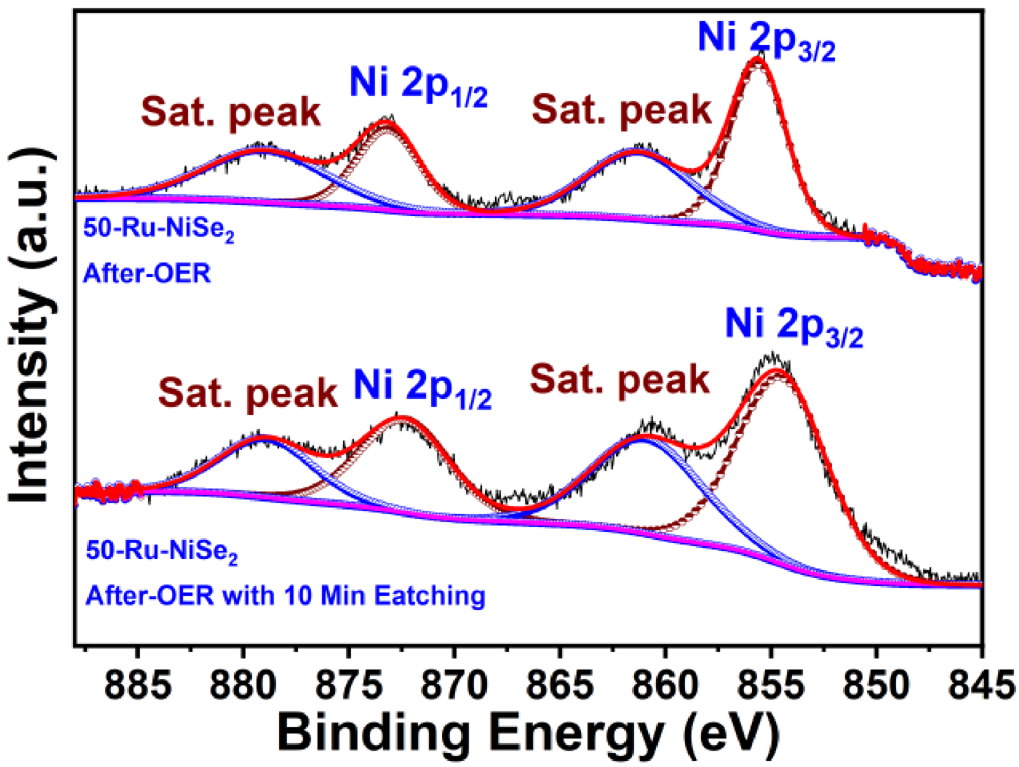

Fig. S8. Post XPS Analysis of Nickel 2p after OER stability test.

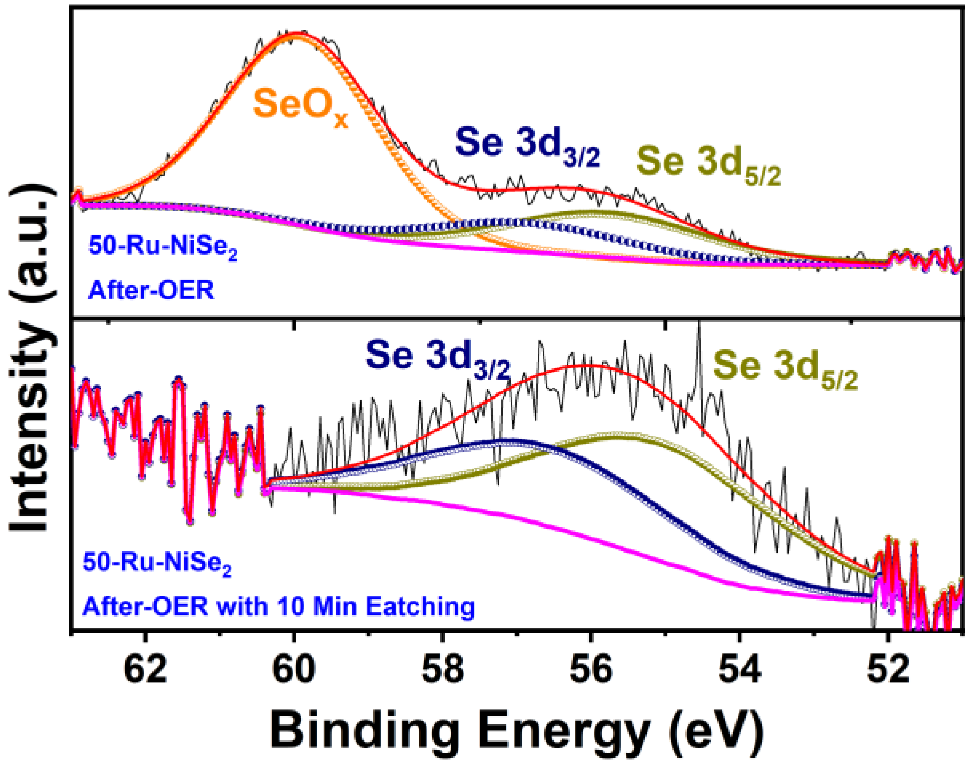

Fig. S9. Post XPS Analysis of Selenium 3d after OER stability test.

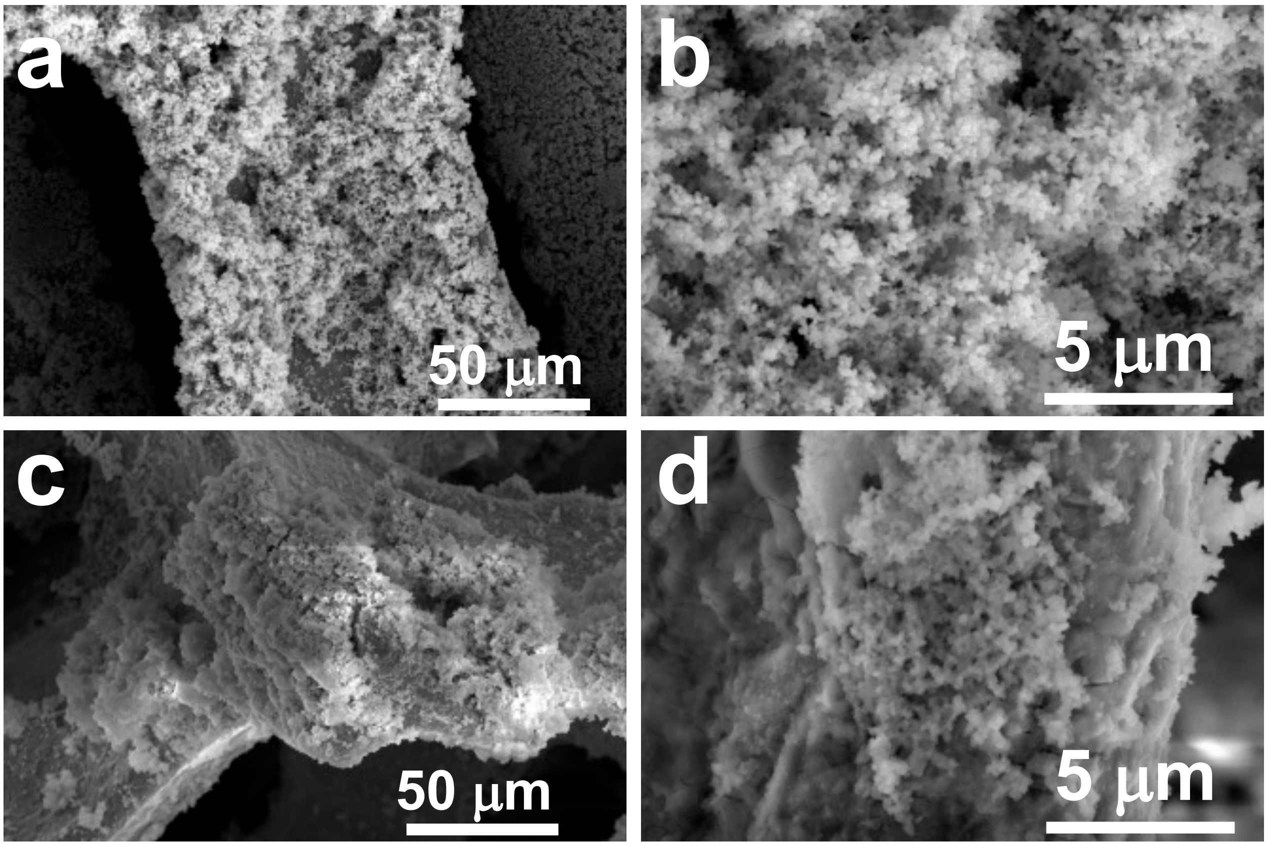

Fig. S10. Comparison between SEM Analysis of 50-Ru-$NiSe_2$ before, after OER stability test. (a-b) SEM image of 50-Ru-$NiSe_2$ before anodic reaction, (a-b) SEM image of 50-Ru-NiSe2 after anodic reaction

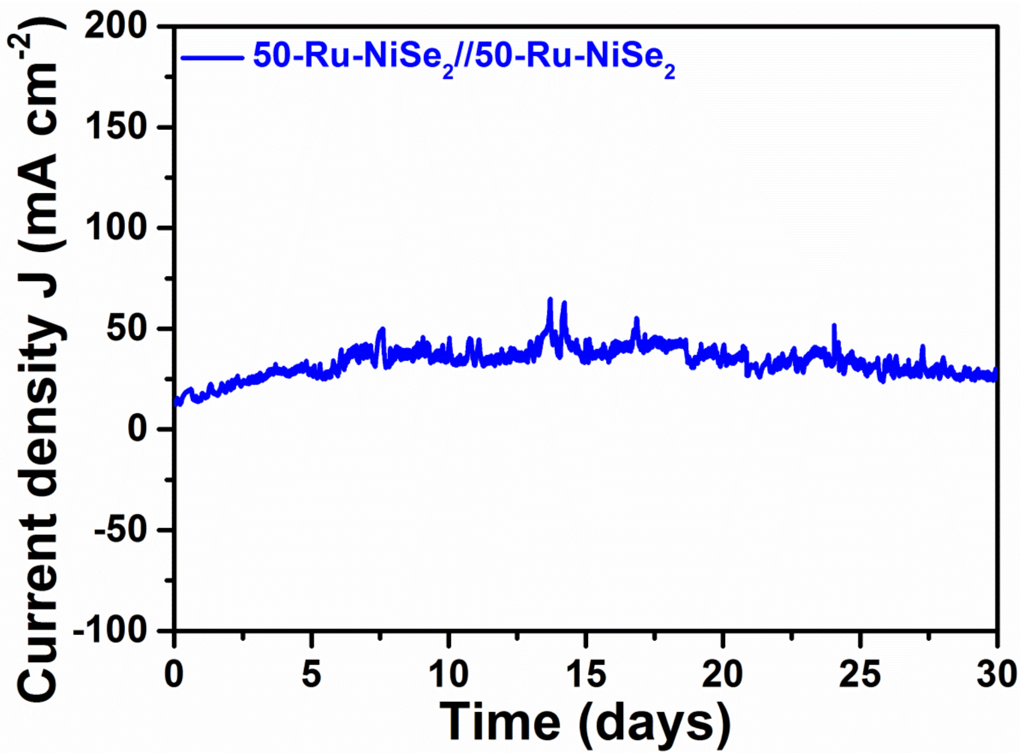

Fig. S11. Chronoamperometry test of 50-Ru-$NiSe_2$//50-Ru-$NiSe_2$ used as both anode and cathode for overall water splitting and it is showing 30 days long-term stability.

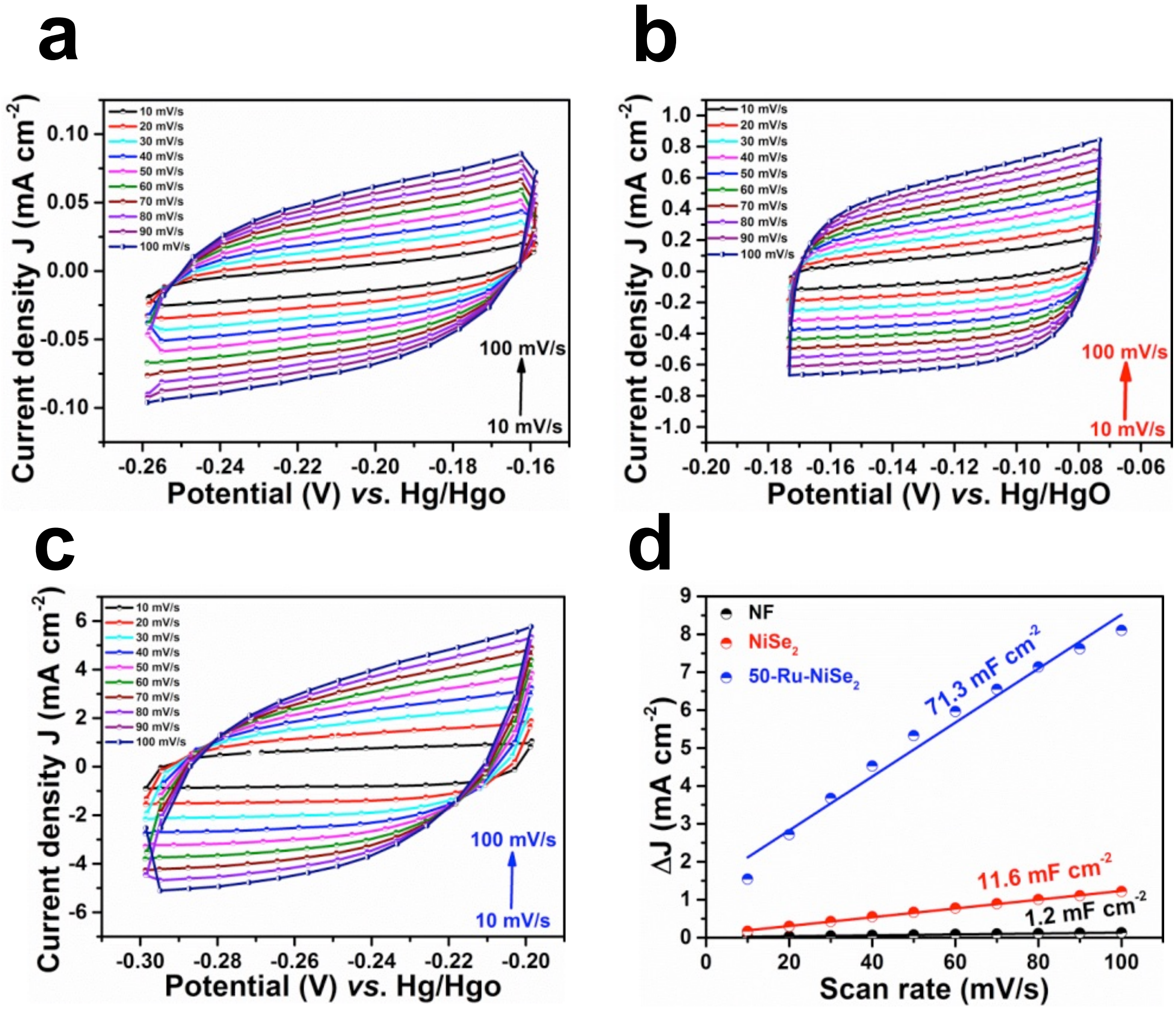

Fig. S12. Cyclic voltammograms in 1 M KOH at different scan rates. (a) Bare nickel foam, (b) $NiSe_2$, (c) 50-Ru-$NiSe_2$, (d) ΔJ *vs.* scan rate plots for C_{dl} calculations.

Note S1. Potential conversion from Hg/HgO to RHE

All potentials were converted to a reversible hydrogen electrode (RHE) by Equation: [1]

$E_{RHE} = E_{Hg/HgO} + E^0_{Hg/HgO} + 0.059 \times pH$

Note S2. Electrical double-layer capacitance (C_{dl}) calculation using cyclic voltammetry (CV) in 1 M KOH

The CVs of $NiSe_2$ and 50-Ru-$NiSe_2$ at different scan rates (10 mV s^{-1} to 100 mV s^{-1}) in 1 M KOH are performed. We plotted ΔJ *vs.* scan rate, and the slope (C_{dl}) is determined from the graph. ECSA was evaluated as,

ECSA = C_{dl}/C_s,

The value of C_s can be taken as 40 μF cm^{-2}.[2]

Table S1. Comparison of the electrocatalytic HER activities of various recently reported electrocatalysts.

S.No	Materials	Overpotential @10 mA cm^{-2}	References
1	Ru-$NiSe_2$	59	Small 2022, 18, 210530500.[3]
2	Ni-MoS_2	112	Small 2022, 18, 2107238.[4]
3	Ru/Co–N–C	23	Adv. Mater. 2022, 34, 2110103.[5]
4	Ni–FeNP (oxide)	46	Nat Commun 2019, 10, 5599.[6]
5	$NiP_2/NiSe_2$	89	Appl. Catal. B 2021, 282, 119584.[7]
6	Fe-Ni_5P_4/NiFeOH	197	Appl. Catal. B 2021,291, 119987. [8]
7	Ni_5P_4-Ru	54	Adv. Mater. 2020, 32, 1906972. [9]
8	Mo-Co_9S_8@C	113	Adv. Energy Mater. 2020, 10, 1903137.[10]

9	MoO_3/Ni–NiO	62	Adv. Mater. 2020, 32, 2003414.[11]
10	W-$NiS_{0.5}Se_{0.5}$	39	Adv. Mater. 2022, 34, 2107053.[12]
11	MoS_2/Ni_3S_2	110	Angew. Chem.Int.Ed 2016, 55, 6702–6707.[13]
12	Co-$ZnRuO_x$	17	Small 2023, 19, 2207235.[14]
13	Ir/MoS_2	44	ACS Energy Lett. 2019, 4, 368−374.[15]
14	CoRu–MoS_2	52	Small 2020, 16, 2000081.[16]
15	Mo_2NiB_2	160	Small 2022, 18, 2104303.[17]
16	Ru-NiCoP/NF	44	Appl. Catal. B 2020, 279, 119396.[18]
17	Co-NC@Mo_2C	99	nano energy 2019, 57, 746-752.[19]
18	Ni-Mo-P	69	Appl. Catal. B 2021, 298, 120494.[20]
19	Ru-MoS_2-Mo_2C	25	nano energy 2021, 88, 106277.[21]
20	$(Ru\text{-}Ni)O_x$	14.5	Appl. Catal. B 2021, 298, 120611.[22]
21	$MoNi_4/MoO_2$	41	nano energy 2023, 109, 108296.[23]
22	Co/CoO/CoN	73	Chemical Eng. J., 2023, 461, 141937.[24]
23	m-NiTPyP	138	Adv. Mater. 2023, 2210727.[25]
24	$Fe_{7.4\%}NiSe$	161	J. Mater. Chem. A, 2019,7, 2233-2241.[26]
25	NiFe-Se/C	160	J. Power Sources, 2017, 366, 193-199. [27]
26	a-$RuTe_2$	36	Nat. Commun. 2019, 10, 5692.[28]
27	$Fe_{0.4}Co_{0.3}Ni_{0.3}$	175	Energy Environ. Mater. 2023, 0, e12590.[29]
28	MnS_xSe_{1-x}@N,F-CQDs	87	Chemical Eng. J. 2023, 459,141610.[30]
29	$Fe_{1-x}Co_xP$	74	Chem. Commun., 2023, 59, 2600-2603.[31]
30	Co/b-Mo_2C@N-CNT	170	Angew. Chem. Int. Ed. 2019, 58, 4923-4928.[32]
31	Ni_3S_2/MoS_2	78	Appl. Catal. B 2020, 268, 118435.[33]

32	NiO@NF-6//Ni_2P@NF-6	99	Nanoscale, 2017, 9, 4409–4418.[34]
33	Ru_1/D-NiFe LDH	18	Nat Commun, 2022, 12, 458.[35]
34	**50-Ru-$NiSe_2$**	**13**	**This Work**

Table S2. OER performance of Ru cluster decorated nickel Diselenide with variously reported catalysts in an alkaline medium..

S.No	Materials	Overpotential @J mA cm^{-2}	References
1	Ru/Co–N–C	247@10 329@100	Adv. Mater. 2022, 34, 2110103.[5]
2	$NiP_2/NiSe_2$	250@10	Appl. Catal. B 2021, 282, 119584.[7]
3	Mo-Co_9S_8@C	200@10	Adv. Energy Mater. 2020, 10, 1903137.[10]
4	MoO_3/Ni–NiO	347@100	Adv. Mater. 2020, 32, 2003414.[11]
5	Co-$ZnRuO_x$	224@10 316@100	Small 2023, 19, 2207235.[14]
6	Ir/MoS_2	330@10	ACS Energy Lett. 2019, 4, 368−374.[15]
7	CoRu–MoS_2	308@10	Small 2020, 16, 2000081.[16]
8	Mo_2NiB_2	280@10	Small 2022, 18, 2104303.[17]
9	Ru-NiCoP/NF	216@20 265@50 285@100	Appl. Catal. B 2020, 279, 119396.[18]
10	Co-NC@Mo_2C	347@10	nano energy 2019, 57, 746-752.[19]
11	Ni-Mo-P	235@10	Appl. Catal. B 2021, 298, 120494.[20]

12	Ru-MoS_2-Mo_2C	280@10	nano energy 2021, 88, 106277.[21]
13	(Ru-Ni)O_x	237.2@10	Appl. Catal. B 2021, 298, 120611.[22]
14	CoNiCH	322@50	Adv. Sci.2023, 2207495.[36]
15	$MoNi_4/MoO_2$	298@10	nano energy 2023, 109, 108296.[23]
16	m-NiTPyP	267@10	Adv. Mater. 2023, 2210727.[25]
17	NiFe-Se/C	240@10 290@50	J. Power Sources, 2017, 366, 193-199.[37]
18	a-$RuTe_2$	285@10	Nat. Commun. 2019, 10, 5692.[28]
19	Co/b-Mo_2C@N-CNT	356@10	Angew. Chem. Int. Ed. 2019, 58, 4923-4928.[32]
20	Ni_3S_2/MoS_2	260@10	Appl. Catal. B 2020, 268, 118435.[33]
21	NiO@NF-6//Ni_2P@NF-6	405@10	Nanoscale, 2017, 9, 4409–4418.[34]
22	Ni/Ni_8P_3 Ni/Ni_8S_3	270@30 340@30	Adv. Funct. Mater., 2016, 26. 3314-3323.[38]
23	**50-Ru-$NiSe_2$**	**260@30**	**This Work**

Table S3. Comparison of the electrocatalytic full cell potential of various recently reported electrocatalysts in 1M KOH at 10 mA cm^{-2}.

S.No	Materials	Overpotential @10 mA cm^{-2}	Ref.
1	Ru-$NiSe_2$	1.537	Small 2022, 18, 2105305.[3]
2	Ni-MoS_2	1.54	Small 2022, 18, 2107238.[4]
3	Ru/Co–N–C	1.50	Adv. Mater. 2022, 34, 2110103.[5]
4	Ni–Fe NP (oxide)	1.47	Nat Commun 2019, 10, 5599.[6]
5	NiP_2/$NiSe_2$	1.56	Appl. Catal. B 2021, 282, 119584.[7]
6	Fe-Ni_5P_4/NiFeOH	1.55	Appl. Catal. B 2021,291, 119987.[8]
7	Ni_5P_4-Ru	--	Adv. Mater. 2020, 32, 1906972.[9]
8	Mo-Co_9S_8@C	1.56	Adv. Energy Mater. 2020, 10, 1903137.[10]
9	MoO_3/Ni–NiO	1.55	Adv. Mater. 2020, 32, 2003414.[11]
10	W-$NiS_{0.5}Se_{0.5}$	1.44	Adv. Mater. 2022, 34, 2107053.[12]
11	MoS_2/Ni_3S_2	1.56	Angew. Chem.Int.Ed 2016, 55, 6702–6707.[13]
12	Co-$ZnRuO_x$	1.48	Small 2023, 19, 2207235.[14]
13	Ir/MoS_2	1.57	ACS Energy Lett. 2019, 4, 368−374.[15]
14	Mo_2NiB_2	1.57	Small 2022, 18, 2104303.[17]
15	Ru-NiCoP/NF	1.515	Appl. Catal. B 2020, 279,119396.[18]
16	Co-NC@Mo_2C	1.685	nano energy 2019, 57, 746-752.[19]
17	Ni-Mo-P	1.46	Appl. Catal. B 2021, 298, 120494.[20]
18	Ru-MoS_2-Mo_2C	1.49	nano energy 2021, 88, 106277.[21]
17	(Ru-Ni)O_x	1.48	Appl. Catal. B 2021, 298, 120611.[22]

20	CoNiCH	1.51	Adv. Sci.2023, 2207495.[36]
21	$MoNi_4/MoO_2$	1.598	nano energy 2023, 109, 108296.[23]
22	Co/CoO/CoN	1.48	Chemical Eng. J., 2023, 461, 141937.[24]
23	m-NiTPyP	1.62	Adv. Mater. 2023, 2210727.[25]
24	$Fe_{7.4\%}$-NiSe	1.58	J. Mater. Chem. A, 2019,7, 2233-2241.[26]
25	NiFe-Se/C	1.68	J. Power Sources, 2017, 366, 193-199.[37]
26	a-$RuTe_2$	1.52	Nat. Commun. 2019, 10, 5692.[28]
27	$Fe_{0.4}Co_{0.3}Ni_{0.3}$	1.62	Energy Environ. Mater. 2023, 0, e12590.[29]
28	MnS_xSe_{1-x}@N,F-CQDs	1.55	Chemical Eng. J. 2023, 459,141610.[30]
29	$Fe_{1-x}Co_xP$	1.59	Chem. Commun., 2023, 59, 2600-2603.[31]
30	Co_3O_4	1.63	Angew. Chem. Int. Ed. 2017, 56, 1324.[39]
31	Co/b-Mo_2C@N-CNT	1.64	Angew. Chem. Int. Ed. 2019, 58, 4923-4928.[32]
32	Ni_3S_2/MoS_2	1.53	Appl. Catal. B 2020, 268, 118435.[33]
33	NiO@NF-6//Ni_2P@NF-6	1.65	Nanoscale, 2017, 9, 4409–4418.[34]
34	Ni/Ni_8P_3	1.61	Adv. Funct. Mater., 2016, 26: 3314-3323.[38]
35	Ru1/D-NiFe LDH	1.44	Nat Commun, 2022, 12, 458.[35]
36	**50-Ru-$NiSe_2$**	**1.45**	**This Work**

Table S4. C_{dl} values were calculated for $NiSe_2$ and 50-Ru-$NiSe_2$.

Catalyst	C_{dl} (mF cm^{-2})
NF	1.2
$NiSe_2$	11.6
50-Ru-$NiSe_2$	71.3

Computational Details

16. Note S3. *Computational Details for density functional theory (DFT) calculations.*

For HER:

The free energy for H adsorption is calculated as:

$$\Delta G_{H*} = E_{ads}(H) + \Delta ZPE_H - T\Delta S_H \quad (1)$$

where, $E_{ads}(H) = E(H^*) - E(*) - E(H_2)$, represents the adsorption energy of the H atom on the surface. $E(H^*)$ and $E(*)$ are the total energies of the surface with and without H and $E(H_2)$ is the total energy of a gas-phase H_2 molecule. The terms ΔZPE_H and ΔS_H account for the difference in zero point energy (ZPE) and entropy between the adsorbed and gas-phase hydrogen, respectively.

We use the fact that vibrational entropy in the adsorbed state is small, approximately equal to half the entropy of a free H_2 molecule, ($S^0_{H_2}$) at standard conditions ($S^0_{H_2}$= 0.41 eV). The values of ΔZPE_H and $T\Delta S_H$ used in our calculations are taken from the literature,[40] resulting in a total contribution of 0.24 eV. Thus, throughout this work, we consider $\Delta G_{H*} = E_{ads}(H) + 0.24$ eV.

Similarly, the free energy of OH adsorption is determined using the equation:

$$\Delta G_{OH*} = E_{ads}(OH) + \Delta ZPE_{OH} - T\Delta S_{OH} \quad (2)$$

In this expression, the total energy of the gas-phase OH is calculated as $E(\mathrm{OH}) = E(\mathrm{H_2O}) - \frac{1}{2}E(\mathrm{H_2})$. The value of $\Delta ZPE - T\Delta S$ for OH adsorption is 0.35 eV, obtained using the respected values given in the literature.[40]\

For OER:

The intermediate reaction steps involved in an OER are as follows:

$* + \mathrm{OH^-} \rightarrow \mathrm{OH^*} + e^-$ (3)

$\mathrm{OH^*} + \mathrm{OH^-} \rightarrow \mathrm{O^*} + \mathrm{H_2O} + e^-$ (4)

$\mathrm{O^*} + \mathrm{OH^-} \rightarrow \mathrm{OOH^*} + e^-$ (5)

$\mathrm{OOH^*} + \mathrm{OH^-} \rightarrow \mathrm{O_2} + * + \mathrm{H_2O} + e^-$ (6)

The free energy change at each of these reaction steps is calculated using the following expressions:

$$\Delta G_1 = G(\mathrm{OH^*}) - G(*) - G(\mathrm{OH^-} - e^-) \quad (7)$$

$$\Delta G_2 = G(\mathrm{O^*}) + G(\mathrm{H_2O}) - G(\mathrm{OH^*}) - G(\mathrm{OH^-} - e^-) \quad (8)$$

$$\Delta G_3 = G(\mathrm{OOH^*}) - G(\mathrm{O^*}) - G(\mathrm{OH^-} - e^-) \quad (9)$$

$$\Delta G_4 = G(*) + G(\mathrm{O_2}) + G(\mathrm{H_2O}) - G(\mathrm{OOH^*}) - G(\mathrm{OH^-} - e^-) \quad (10)$$

While calculating these ΔG values, we consider the following factors:

- The free energy of the adsorbed species is calculated as: $\Delta G = E_{ads} + \Delta ZPE - T\Delta S$. Here, the total energies of the surface before and after the adsorption, as well as those of the free species, are obtained from DFT calculations. The entropy contribution primarily comes from the gas-phase species, while the contribution from the adsorbed species is negligible.

- The value of $G(H_2O(l))$ is assumed to be equal to the free energy of gas-phase H_2O molecule at 300 K and 0.035 bar of pressure, where they are in equilibrium. The ΔZPE and $T\Delta S$ corrections are taken from the literature.40
- Since DFT tends to overestimate the binding energy of a gas-phase O_2 molecule, we calculated its free energy by using the expression: $E(O_2) = 2E(H_2O) - 2E(H_2)$.
- The value of $G(OH^- - e^-)$ is determined using the equation: $G(OH^- - e^-) = G(H_2O(l)) - 1/2G(H_2) + eU + \ln(10) * k_B T * pH$, as suggested by Liu et al.[42] Here, U is the applied potential, e denotes the magnitude of the electronic charge, and pH refers to the pH value of the electrochemical environment. We assume U=0 and consider the last term involving pH to be zero, ensuring that the potentials obtained from free energy calculations are referenced to the RHE electrode.

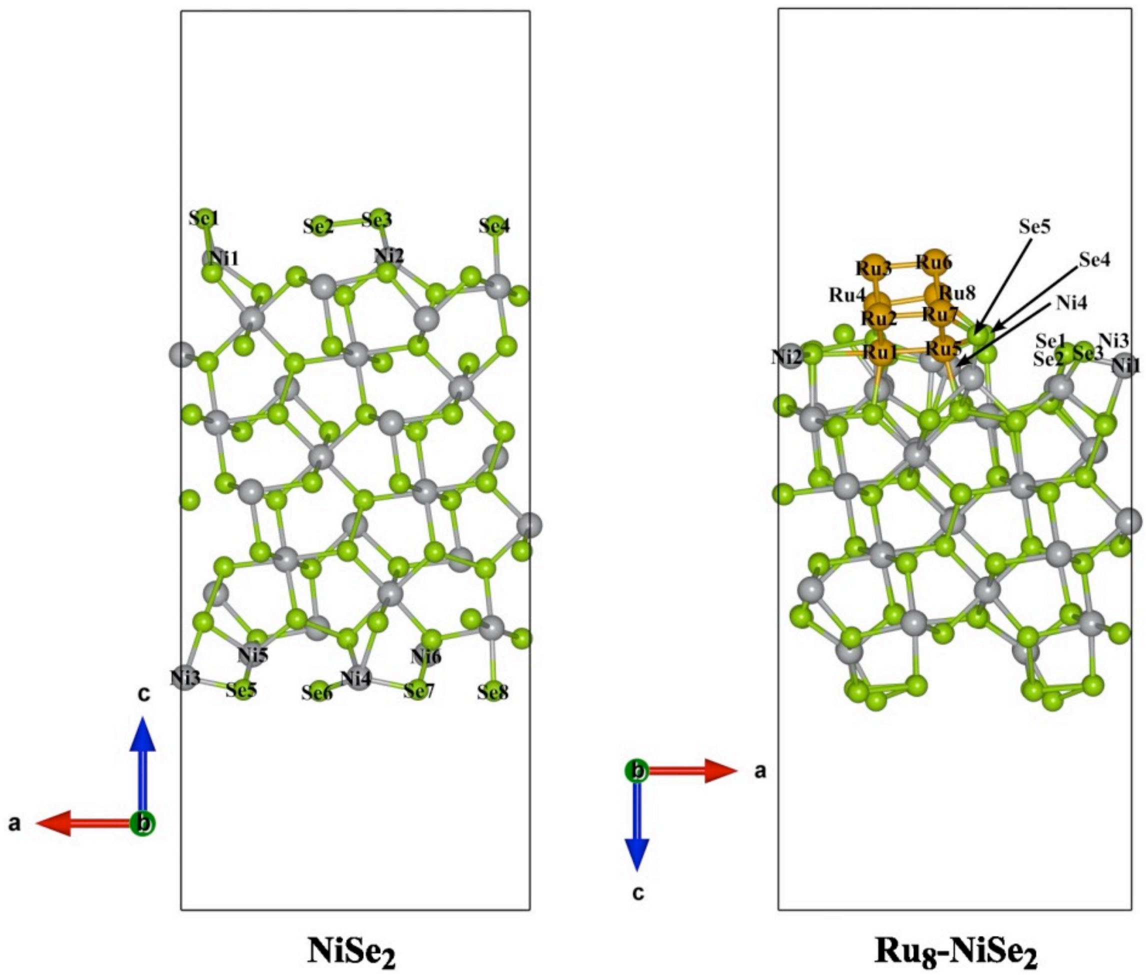

Fig. S13. Crystal structures of studied samples. Side-view of the structures of pristine and Ru_8-$NiSe_2$(210) systems. Green, grey, and golden-yellow-colored balls represent Se, Ni, and Ru atoms, respectively.

Table S5. Adsorption energy, $E_{ads}(H_2O)$, of a H_2O molecule at various possible sites of $NiSe_2(210)$ and Ru_8-$NiSe_2(210)$ surfaces.

System	$E_{ads}(H_2O)$	Relaxed position of H_2O
$NiSe_2$	−0.50	Ni1 - top
	−0.35	Ni2 - top
	−0.83	Ni3 - top
	−0.60	Ni4 - top
	−0.51	Ni5 - top
	−0.45	Ni6 - top
Ru_8-$NiSe_2$	−1.08	Ru6 - top
	−0.87	Ru3 - top
	−0.60	Ru4 - top
	−0.54	Ni3 - top
	−0.51	Ru8 - top
	−0.38	Ni4 - top

Table S6. Adsorption free energy, ΔG_{OH*}, of OH at various possible sites of $NiSe_2(210)$ and Ru_8-$NiSe_2(210)$ surfaces.

System	ΔG_{OH*}	Relaxed position of OH
$NiSe_2$	0.97	Se2 - top
	0.86	Ni1 - top
	1.03	Ni2 - top
	1.04	Ni3 - top
	1.04	Ni4 - top
	0.90	Ni5 - top
	0.90	Ni6 - top
Ru_8-$NiSe_2$	−0.97	Ru2-Ru3 bridge
	−0.53	Ru6-top
	−0.28	Ru3-top
	0.02	Ru3-Ru4 bridge
	0.02	Ru4 - top
	0.04	Ru3-Ru6 bridge

	0.23	Ru8-top
	0.51	Ru6-Ru7 bridge

Table S7. Calculated values of ΔG (in eV) for intermediate steps of OER and η (in V) at various sites of $NiSe_2(210)$ and Ru_8-$NiSe_2(210)$ surfaces.

System	**Site**	ΔG_1	ΔG_2	ΔG_3	ΔG_4	**η**
$NiSe_2$	Se1-top	1.13	1.01	2.24	0.54	1.01
	Se2-top	0.97	0.67	2.74	0.54	1.51
	Se3-top	1.13	1.01	2.11	0.67	0.88
	Se4-top	1.09	0.55	2.82	0.46	1.59
	Se6-top	1.41	-0.32	3.53	0.30	2.30
	Se8-top	1.38	-0.29	3.54	0.29	2.31
Ru_8-$NiSe_2$	Ru3-top	-0.28	0.39	2.66	2.15	1.43
	Ru4-top	0.02	-0.02	3.19	1.73	1.96
	Ru6-top	-0.53	0.43	2.87	2.15	1.64
	Ru8-top	0.23	0.48	2.44	1.77	1.21

Ru2-Ru7 bridge	1.01	0.30	2.96	0.65	1.73
Se1-top	1.30	0.12	2.92	0.58	1.69
Se2-top	1.09	1.15	2.02	0.66	0.79
Se3-top	1.14	0.85	2.41	0.52	1.18

References

1 N. P. Dileep, P. V. Sarma, R. Prasannachandran, V. Surendran and M. M. Shaijumon, *ACS Appl Nano Mater*, 2021, **4**, 7206–7212.

2 N. P. Dileep, T. V. Vineesh, P. V. Sarma, M. V. Chalil, C. S. Prasad and M. M. Shaijumon, *ACS Appl Energy Mater*, 2020, **3**, 1461–1467.

3 R. Qin, P. Wang, Z. Li, J. Zhu, F. Cao, H. Xu, Q. Ma, J. Zhang, J. Yu and S. Mu, *Small*, , DOI:10.1002/smll.202105305.

4 G. Wang, G. Zhang, X. Ke, X. Chen, X. Chen, Y. Wang, G. Huang, J. Dong, S. Chu and M. Sui, *Small*, , DOI:10.1002/smll.202107238.

5 C. Rong, X. Shen, Y. Wang, L. Thomsen, T. Zhao, Y. Li, X. Lu, R. Amal and C. Zhao, *Advanced Materials*, , DOI:10.1002/adma.202110103.

6 B. H. R. Suryanto, Y. Wang, R. K. Hocking, W. Adamson and C. Zhao, *Nat Commun*, , DOI:10.1038/s41467-019-13415-8.

7 L. Yang, L. Huang, Y. Yao and L. Jiao, *Appl Catal B*, , DOI:10.1016/j.apcatb.2020.119584.

8 C. F. Li, J. W. Zhao, L. J. Xie, J. Q. Wu and G. R. Li, *Appl Catal B*, , DOI:10.1016/j.apcatb.2021.119987.

9 Q. He, D. Tian, H. Jiang, D. Cao, S. Wei, D. Liu, P. Song, Y. Lin and L. Song, *Advanced Materials*, , DOI:10.1002/adma.201906972.

10 L. Wang, X. Duan, X. Liu, J. Gu, R. Si, Y. Qiu, Y. Qiu, D. Shi, F. Chen, X. Sun, J. Lin and J. Sun, *Adv Energy Mater*, , DOI:10.1002/aenm.201903137.

11 X. Li, Y. Wang, J. Wang, Y. Da, J. Zhang, L. Li, C. Zhong, Y. Deng, X. Han and W. Hu, *Advanced Materials*, , DOI:10.1002/adma.202003414.

12 Y. Wang, X. Li, M. Zhang, J. Zhang, Z. Chen, X. Zheng, Z. Tian, N. Zhao, X. Han, K. Zaghib, Y. Wang, Y. Deng and W. Hu, *Advanced Materials*, , DOI:10.1002/adma.202107053.

13 J. Zhang, T. Wang, D. Pohl, B. Rellinghaus, R. Dong, S. Liu, X. Zhuang and X. Feng, *Angewandte Chemie*, 2016, **128**, 6814–6819.

14 D. Liu, Z. Wu, J. Liu, H. Gu, Y. Li, X. Li, S. Liu, S. Liu and J. Zhang, *Small*, , DOI:10.1002/smll.202207235.

15 S. Wei, X. Cui, Y. Xu, B. Shang, Q. Zhang, L. Gu, X. Fan, L. Zheng, C. Hou, H. Huang, S. Wen and W. Zheng, *ACS Energy Lett*, 2019, **4**, 368–374.

16 I. S. Kwon, T. T. Debela, I. H. Kwak, Y. C. Park, J. Seo, J. Y. Shim, S. J. Yoo, J. G. Kim, J. Park and H. S. Kang, *Small*, , DOI:10.1002/smll.202000081.

17 A. Saad, Y. Gao, K. A. Owusu, W. Liu, Y. Wu, A. Ramiere, H. Guo, P. Tsiakaras and X. Cai, *Small*, , DOI:10.1002/smll.202104303.

18 D. Chen, R. Lu, Z. Pu, J. Zhu, H. W. Li, F. Liu, S. Hu, X. Luo, J. Wu, Y. Zhao and S. Mu, *Appl Catal B*, , DOI:10.1016/j.apcatb.2020.119396.

19 Q. Liang, H. Jin, Z. Wang, Y. Xiong, S. Yuan, X. Zeng, D. He and S. Mu, *Nano Energy*, 2019, **57**, 746–752.

20 B. Zhang, F. Yang, X. Liu, N. Wu, S. Che and Y. Li, *Appl Catal B*, , DOI:10.1016/j.apcatb.2021.120494.

21 V. H. Hoa, D. T. Tran, S. Prabhakaran, D. H. Kim, N. Hameed, H. Wang, N. H. Kim and J. H. Lee, *Nano Energy*, 2021, **88**, 106277.

22 H. Zhang, Y. Lv, C. Chen, C. Lv, X. Wu, J. Guo and D. Jia, *Appl Catal B*, , DOI:10.1016/j.apcatb.2021.120611.

23 X. Meng, Z. Li, Y. Liu, Z. Wang, P. Wang, Z. Zheng, Y. Dai, B. Huang, H. Cheng and J.-H. He, *Nano Energy*, 2023, **109**, 108296.

24 W. Zhang, C. Li, J.-Y. Ji, Z. Niu, H. Gu, B. F. Abrahams and J.-P. Lang, *Chemical Engineering Journal*, 2023, **461**, 141937.

25 Y. Zhang, S. Chen, Y. Zhang, R. Li, B. Zhao and T. Peng, *Advanced Materials*, 2023, 2210727.

26 Z. Zou, X. Wang, J. Huang, Z. Wu and F. Gao, *J Mater Chem A Mater*, 2019, **7**, 2233–2241.

27 B. Xu, H. Yang, L. Yuan, Y. Sun, Z. Chen and C. Li, *J Power Sources*, 2017, **366**, 193–199.

28 J. Wang, L. Han, B. Huang, Q. Shao, H. L. Xin and X. Huang, *Nat Commun*, , DOI:10.1038/s41467-019-13519-1.

29 Y. Chen, L. Yang, C. Li, Y. Wu, X. Lv, H. Wang and J. Qu, *Energy and Environmental Materials*, , DOI:10.1002/eem2.12590.

30 B. Sun, G. Dong, J. Ye, D. feng Chai, X. Yang, S. Fu, M. Zhao, W. Zhang and J. Li, *Chemical Engineering Journal*, , DOI:10.1016/j.cej.2023.141610.

31 S. Marimuthu, A. Shankar and G. Maduraiveeran, *Chemical Communications*, 2023, **59**, 2600–2603.

32 T. Ouyang, Y. Ye, C. Wu, K. Xiao and Z. Liu, *Angewandte Chemie*, 2019, **131**, 4977–4982.

33 C. Wang, X. Shao, J. Pan, J. Hu and X. Xu, *Appl Catal B*, , DOI:10.1016/j.apcatb.2019.118435.

34 J. Zheng, W. Zhou, T. Liu, S. Liu, C. Wang and L. Guo, *Nanoscale*, 2017, **9**, 4409–4418.

35 P. Zhai, M. Xia, Y. Wu, G. Zhang, J. Gao, B. Zhang, S. Cao, Y. Zhang, Z. Li, Z. Fan, C. Wang, X. Zhang, J. T. Miller, L. Sun and J. Hou, *Nat Commun*, 2021, **12**, 4587.

36 T. Zeng, B. Guo, Z. Xu, F. Mo, X. Chen, L. Wang, Y. Ding and J. Bai, *Advanced Science*, , DOI:10.1002/advs.202207495.

37 B. Xu, H. Yang, L. Yuan, Y. Sun, Z. Chen and C. Li, *J Power Sources*, 2017, **366**, 193–199.

38 G. F. Chen, T. Y. Ma, Z. Q. Liu, N. Li, Y. Z. Su, K. Davey and S. Z. Qiao, *Adv Funct Mater*, 2016, **26**, 3314–3323.

39 Y. P. Zhu, T. Y. Ma, M. Jaroniec and S. Z. Qiao, *Angewandte Chemie*, 2017, **129**, 1344–1348.

40 J. K. Nørskov, T. Bligaard, A. Logadottir, J. R. Kitchin, J. G. Chen, S. Pandelov and U. Stimming, *J Electrochem Soc*, 2005, **152**, J23.

41 A. Hellman and R. G. S. Pala, *The Journal of Physical Chemistry C*, 2011, **115**, 12901–12907.

42 S. Liu, M. G. White and P. Liu, *The Journal of Physical Chemistry C*, 2016, **120**, 15288–15298.